UKAEA FUS 398

UKAEA Fusion
(UKAEA/Euratom Fusion Association)

MHD Beta Limit for Peaked Pressure Profile Reversed Magnetic Shear Equilibria

O J Kwon, T C Hender, G Huysmans

May 1998 28p. A CA

UKAEA
Fusion

Culham Science Centre, Abingdon
Oxfordshire, OX14 3DB
United Kingdom
Telephone +44 1235 464216
Facsimile +44 1235 463647

MHD Beta Limit for Peaked Pressure Profile Reversed Magnetic Shear Equilibria

O. J. Kwon,* T. C. Hender
UKAEA Fusion, Culham Science Centre
Abingdon, Oxfordshire
Euratom-UKAEA Fusion Association
United Kingdom

G. T. A. Huysmans
JET Joint Undertaking
Abingdon, Oxon, OX14 3EA, UK

May 1, 1998

Abstract

The ideal MHD β limit of reversed shear equilibria, due to $n = 1$, 2, and ballooning modes, is investigated for peaked pressure profiles, consistent with those occuring when the internal transport barrier is estabilished in JET optimised shear discharges. Higher β_N can be reached with the control of the minimum q value and a conducting wall can further improve the stable domain. The $n = 2$ mode plays an insignificant role, unless the conducting wall improves the $n = 1$ stability when the shear reversal is large. Increasing the amount of shear reversal generally improves MHD stability and the effect is stronger for the $n = 2$ mode. β^* $(=2\mu_0 < P^2 >^{1/2}/B_0^2)$ increases with normalised current (I_p/aB_0) but β_N is only weakly affected.

*permanent address : Department of Physics, Taegu University, Kyungbook, Republic of Korea

1 Introduction

Recently, an interest in reversed magnetic shear equilibria in tokamaks has been renewed both experimentally and theoretically. It has long been recognised that equilibria with a hollow q-profile, where q is the safety factor, can support a large pressure gradient in the negative magnetic shear region because ballooning modes enter the second stable regime [1]. Also, a large bootstrap current fraction, which is important for steady-state operation of the tokamak, leads to hollow current profiles and to reversed shear equilibria due to the lack of trapped particles in the core.

High performance with reversed shear has been observed transiently in DIII-D [2], JET [3], TFTR [4], and JT-60U [5], with an early application of heating power in the current ramp-up phase of the discharge to inhibit current penetration. It was found that β_N as high as 4 could be reached in DIII-D [2], while for very peaked pressure profiles in JET, MHD stability limits β_N to less than 1.8 [6, 7]. Here, β_N is the normalised beta or the Troyon coefficient [8], defined as

$$\beta_N = \beta_t(\%)\frac{a(m)B_0(T)}{I_p(MA)},$$

$$\beta_t = \frac{2\mu_0 \int P\, dS}{B_0^2 \int dS},$$

where dS denotes the surface elements of the plasma cross section, B_0 the vacuum magnetic field at the geometric axis, a the minor radius, I_p the plasma current, and P is the plasma pressure. In these experiments, where the current profile is controlled, internal transport barriers have been formed and ion heat conduction has been greatly reduced, possibly by suppressing microinstabilities due to $\vec{E} \times \vec{B}$ flow shear [9] or negative shear [10]. The improved confinement leads to quite peaked pressure profiles. A peaked

pressure profile is favourable because the fusion power is roughly proportional to P^2, and so the fusion power increases approximately linearly with P_f for the same β_t, where $P_f = P_0 \int dS / \int dS\, P$ is the pressure peaking factor and P_0 is the pressure on axis. However, peaked pressure profile discharges face disruptions due to low-n MHD instabilities [6, 7] if β_N increases further without broadening of the pressure profile.

It is important to understand and improve the MHD stability limit of reversed shear equilibria. In TFTR with circular cross section, it was found [11] that increasing $\Delta q = q_0 - q_{\min}$ (where q_0 and $q_{\min}$ are the central q, and minimum q value respectively) and the radius of shear reversal, has a stronger effect on stabilising $n \geq 2$ modes than the $n = 1$ mode and that the wall has a limited effect for a peaked pressure profile. In D-shaped plasmas, broader pressure profiles, strong shaping and a conducting wall have a synergistic effect [12, 13, 14] and can increase β_t by a factor of up to 5, compared with a circular plasma with a peaked pressure. Similar results were found [15] with different forms of pressure and q profiles. When reversed shear equilibria have been stabilised to ideal low n modes (without a conducting wall), high n ideal ballooning modes [17] and resistive interchange modes [18], the maximum β_N is reached for $q_{\min} \simeq 1.2$, with P_f between 2.5 and 3 [16]. This broad pressure profile gives a better aligned bootstrap current, but it does not match the profiles observed in high performance reversed shear experiments [2, 3, 4].

In this study, we investigate the effect of $q_{\min}$, Δq, the conducting wall and the total current on the β limit due to the ideal $n = 1$, 2 and ballooning modes for JET type plasmas. Here, the pressure profiles are quite peaked, consistent with L-mode optimised shear operation in JET, where the internal transport barrier is at $q \simeq 2$ surface [7] This study is complementary to

previous findings [12, 13, 14, 15, 16].

The remainder of this paper is organised as follows. Section 2 describes how reversed shear equilibria, which match the JET experiment, are generated to determine MHD stability in the $\beta - q_{\min}$ space. Section 3 contains numerical results and explanations. Conclusions and a discussion are given in Section 4.

2 Numerical Model

The HELENA code [19] is used to generate the numerical equilibria and to determine ballooning mode stability. A fixed boundary, up-down symmetric D-shaped plasma, with elongation 1.7 and triagularity 0.3 at an aspect ratio of 0.315, is used. This boundary shape approximates that of JET reversed shear plasmas though they have single null X-points. Some stability calculations using a JET-like single null equilibria are presented to show that the up-down symmetrisation of the boundary makes no significant difference. The pressure profile is chosen to match the experimental pressure profile of JET shot #40847 at 47.0sec. This pressure profile is modelled by

$$\frac{dP}{d\Psi} = A\left[0.25\left(1-\frac{\Psi}{\Psi_a}\right)^2 + \left(1-\frac{\Psi}{\Psi_a}\right)^6\right],$$

where Ψ_a is the value of the poloidal flux function Ψ the at edge and A is the parameter used to vary β. The pressure profile is quite peaked as shown in Fig. 1(d), consistent with the internal transport barrier in JET. The equilibrium profile is then determined by specifying

$$\frac{dP}{d\Psi} + \frac{\mu_0}{R_0^2} F \frac{dF}{d\Psi} = \sum_{i=1, i\neq 5}^{7} B_i \left(1-\frac{\Psi}{\Psi_a}\right)^i,$$

where B_i's are parameters used to vary the current profile, i.e., changing $q_{\min}$ at fixed q_a. The imposed conditions make the toroidal current vanish

at the plasma boundary. Typical pressure and q profiles are shown in Fig. 1, corresponding to the range of equilibria used in this paper.

The choice of the method of generating numerical equilibria makes P_f, Δq, and the radial position of $q_{\min}$ vary as β_N and $q_{\min}$ are changed. In particular, P_f changes because of the large Shafranov shift of the magnetic axis at high β. It varies from 4.8 to 5.8 in the range of this study and decreases with $q_{\min}$, and also slightly with β. However, this parametrisation covers a wide range of $q_{\min}$ and β, enabling us to investigate MHD stability of reversed shear equilibria, at relatively low q_a. It should be noted that simple equilibria with very high q_0 at large β are hard to generate, because the large $dP/d\Psi$ contribution on the toroidal current at the centre tends to make the q profile have double minima. This limits the range of the $\beta - q_{\min}$ space in this study.

The ideal MHD stability limit due to low n modes is determined by using the MISHKA-1 code [20]. Generally, a total of 21 poloidal modes ($-2 \leq m \leq 18$ for the $n = 1$ mode, and $-1 \leq m \leq 19$ for the $n = 2$ mode, where m is the poloidal mode number) were used to find the growth rate of the mode. In some cases, the number and range of modes has been changed to check convergence. A conducting wall outside a plasma with toroidal rotation, as confirmed experimentally [21], will favorably affect the stability of low-n MHD modes. We have considered the effect of normalised wall positions (r_{wall}) of 1.15 and 1.3 times the local plasma radius. This is representative of the likely wall location for the complex structure surrounding the plasma in JET.

3 Numerical Results

The β limits due to the $n = 1$ mode, are shown in terms of β^* as a function of $q_{\min}$ in Fig. 2. Here,

$$\beta^* = \frac{2\mu_0(\int P^2\, dS \,/\, \int dS\,)^{1/2}}{B_0^2},$$

which gives a measure of the fusion efficiency (fusion power is roughly proportional to P^2 for the temperature range of interest). The edge q value (q_a) is fixed at 4.5, unless noted otherwise. In Fig. 2, $B_1 = B_4 = B_6 = 0$ are used. The q-profile of an equilibrium that is marginally stable to the $n = 1$ mode with $r_{\rm wall} = 1.3$ at $q_{\min} \simeq 1.34$ is shown in Fig. 1(a). It should be noted that Δq and the location of $q_{\min}$ also change with $q_{\min}$ as shown in Fig. 3(a), where values are shown along the $n = 1$ stability limit with $r_{\rm wall} = 1.3$ in Fig. 2. The location of $q_{\min}$ is shown in terms of an effective normalised minor radius $\sqrt{\Psi_{\min}/\Psi_a}$, where $\Psi_{\min}$ is the poloidal flux function at the $q_{\min}$ surface. It can be seen that both Δq and $\sqrt{\Psi_{\min}/\Psi_a}$ increase with $q_{\min}$. However, the change in I_p/aB_0 is negligible ($1.08 \leq I_p/aB_0 \leq 1.11$) as q_a is held fixed.

The β limit due to the $n = 1$ mode improves rapidly as $q_{\min}$ is raised above 1, as shown in Fig. 2, since the $q = 1$ surface is removed from the plasma. The β limit due to the $n = 1$ mode without the wall reaches a local maximum at $q_{\min} \simeq 1.3$, where $\Delta q \simeq 0.7$, $\beta_t \simeq 2.6\%$, $\beta_N \simeq 2.4$, and $\beta^* \simeq 4.2\%$, can be achieved. Here, β_N is lower than the Troyon limit for a monotonic q-profile, but the strong peaking of the pressure gives rise to high β^* (i.e., a high potential fusion power). It is interesting to recall that the MHD limit in recent JET reversed shear experiments was $\beta_N \simeq 1.8$ [7]. Therefore, improvement is expected if the q profile can be controlled, even without the wall stabilisation. The maximum β_N is also lower than the limit

with a broad pressure profile [16] in reversed shear, as expected because broad pressure is favorable for $n = 1$ stability [11, 13].

The mode structure at low $q_{\min}$ (Fig. 4(a)) shows large internal $m = 1$ and $m = 2$ components, even if the rational $q = 1$ surface is not present. This is why the effect of the wall is small at low $q_{\min}$. However, at higher $q_{\min}$, contributions from modes with high m numbers as shown in Fig. 4(b), become larger and have significant external components at the plasma boundary. Therefore, the conducting wall has a stronger stabilising effect for higher $q_{\min}$ equilibria. The wall stabilisation as shown in Fig. 2 for $q_{\min} \geq 1.2$ is consistent with previous results, i.e., the conducting wall is effective for D-shaped cross sections as in D-IIID [13], while the effect is much less significant for circular plasmas such as TFTR [11]. We note that different reversed shear equilibria with broader pressure and large q_a were used in Ref. [13]. Since the local maximum β due the $n = 1$ mode without a wall is limited by a mode with large external components at higher $q_{\min}$; it increases significantly as a conducting wall is fitted. Further investigation of the β limit for larger $q_{\min}$ outside the range shown in Fig. 2 is hampered by the appearance of double minima in the q-profile. For $r_{\text{wall}} = 1.3$, an equilibrium with $\beta_t \simeq 3.2\%$, $\beta_N \simeq 2.9$, and $\beta^* \simeq 5.1\%$, at $q_{\min} \simeq 1.45$, is stable to the $n = 1$ external kink mode, but is $n = 2$ unstable. For a closer wall ($r_{\text{wall}} = 1.15$), the β limit shown in Fig. 2 does not saturate, and $\beta_t \simeq 3.7\%$, $\beta_N \simeq 3.3$, and $\beta^* \simeq 5.9\%$, are reached. With the JET experimental boundary shape (as shown in the inset of Fig. 2) with a single null X-point, the β^* limit, which is denoted by crosses, is in good qualitative agreement with the up-down symmetrised results; $r_{\text{wall}} = 1.3$ is used for these points.

The initial increase in β^* for the $n = 2$ mode when $q_{\min}$ is raised above 1, is steeper than that of the $n = 1$ mode as shown in Fig. 5. After the $n = 2$ β^*

limit reaches a local maximum when $q_{\min} \simeq 1.15$, it decreases as $q_{\min}$ gets close to another rational surface, i.e., $m = 3/n = 2$, and then increases again when $q_{\min}$ is further raised. Over a wide range of $q_{\min}$, the mode structure is dominated by large $m = 2$, 3 components, which are mainly internal, as shown in Fig. 6. Therefore, the effect of wall stabilisation on the $n = 2$ mode, with $r_{\text{wall}} = 1.3$ (Fig. 5), is smaller than that on the $n = 1$ mode (Fig. 2). The $n = 2$ limit is well above the $n = 1$ limit without the conducting wall, but for the more realistic $r_{\text{wall}} = 1.3$, the $n = 2$ mode sets a lower β^* limit than the $n = 1$ mode for $q_{\min} \geq 1.33$. With $r_{\text{wall}} = 1.15$, the $n = 2$ mode limits the increase of β^* well before the maximum due to the $n = 1$ mode is reached.

Ballooning modes are stabilised rapidly as $q_{\min}$ is raised, as shown in Fig. 5. This improvement is largely due to increased potential well stabilisation when the local q increases. Flux surfaces which first become unstable to ballooning modes are in the low positive shear region just outside the $q_{\min}$ surface. Since the ballooning β^* limit can be improved by lowering the pressure gradient locally in that region, it is not considered as a hard limit. The ballooning modes only affect a small region. This is illustrated in Fig. 6 which also shows the β^* limit when 10% of the surfaces are ballooning unstable, where β^* improves considerably. This limit is generally above other MHD limits.

Figure 7 shows β^* limits with the condition $B_1 = B_4 = B_7 = 0$. The q-profile for these parameters is less hollow and $\sqrt{\Psi_{\min}/\Psi_a}$ only slightly decreases, as shown in Fig. 3(b), compared with the previous case (Fig. 3(a)); again these parameters are shown along the $n = 1$, $r_{\text{wall}} = 1.3$ stability boundary. The q-profile of an equilibrium that is marginally stable to the $n = 1$ mode with $r_{\text{wall}} = 1.3$ at $q_{\min} \simeq 1.34$ is shown in Fig. 1(b). The

behaviour of the β^* limits given by $n = 1$, 2, and ballooning modes remains qualitatively unchanged, i.e., the $n = 2$ limit is unimportant unless there is a conducting wall, and ballooning modes set the soft β limit for low $q_{\min}$. A local maximum of the $n = 1$ mode stability without the conducting wall, ($\beta_t \simeq 2.5\%$, $\beta_N \simeq 2.3$, and $\beta^* \simeq 4.2\%$) is reached when $q_{\min} \simeq 1.34$ and $\Delta q \simeq 0.5$. With $r_{\text{wall}} = 1.3$, the β limit improves and $\beta_t \simeq 3.0\%$, $\beta_N \simeq 2.7$, and $\beta^* \simeq 4.9\%$ can be achieved when $q_{\min} \simeq 1.37$. This local maximum is a lot broader than that without the wall, which means that detailed control of the current is not needed to maintain stability. When $r_{\text{wall}} = 1.15$, an $n = 1$ stable equilibrium, $\beta_t \simeq 3.7\%$, $\beta_N \simeq 3.3$, and $\beta^* \simeq 5.9\%$, is possible. Compared with Fig. 5, the local minimum β^* limit due to the $n = 2$ mode near $q_{\min} \simeq 1.5$ drops closer to the β^* boundary of $n = 1$ mode without a wall, and the ballooning mode stability deteriorates.

In Fig. 8, results are shown when the plasma current is varied by specifying $B_4 = B_7 = 0$, $B_2 = 4B_1$. The q-profiles along the $n = 1$ stability boundary with $r_{\text{wall}} = 1.3$ are only slightly hollow and the location of $q_{\min}$ has moved inwards as shown in Fig. 3(c), such that $\sqrt{\Psi_{\min}/\Psi_a}$ has decreased by about 10% compared to the case used to generate Fig. 2 for the same $q_{\min}$. The q-profile of an equilibrium that is marginally stable to the $n = 1$ mode with $r_{\text{wall}} = 1.3$ at $q_{\min} \simeq 1.34$ is shown in Fig. 1(c). The noticeable difference due to the less hollow q, is that the $n = 2$ mode now sets the β^* limit just after the $n = 1$ no wall case passes the local maximum at $q_{\min} \simeq 1.37$, with $\beta_t \simeq 2.3\%$, $\beta_N \simeq 2.2$, and $\beta^* \simeq 3.9\%$. We note it was also found [11] for the circular tokamak, that higher n modes are more easily affected by the change of profiles like Δq, while the $n = 1$ limit is only modestly affected. With $r_{\text{wall}} = 1.3$, the β limit due to the $n = 1$ mode reaches $\beta_t \simeq 2.7\%$, $\beta_N \simeq 2.5$, and $\beta^* \simeq 4.4\%$. This decreases slightly when the $n = 2$ mode

is considered simultaneously, due to the broadness of the $n = 1$ maximum. However, the nearly saturated limit of $\beta_t \simeq 3.7\%$, $\beta_N \simeq 3.3$, and $\beta^* \simeq 5.0\%$ with $r_{\rm wall} = 1.15$ is reduced by 14% due to the lower $n = 2$ limit.

The effect of raising the amount of shear reversal can be investigated by comparing Figs. 2, 5, 7, and 8. In general, the β^* limit improves as Δq increases for all ideal MHD modes in the range considered here, but saturates for larger $\Delta q (\geq 0.5)$. For the $n = 1$ mode limit without a wall, the $q_{\rm min}$ value where it reaches a local maximum decreases slightly and the peak β^* rises from 3.7% to 4.2% when Δq is raised from 0.1 to 0.7, at $q_{\rm min} \simeq 1.3$. The presence of the wall and raising Δq have the additional effect of improving the β^* limit of the $n = 1$ mode for $q_{\rm min} \geq 1.3$, where the mode has a more external character, and acts to increase and broaden the β boundary near the local maximum. The effect of changing Δq is greater for the $n = 2$ mode over the whole $q_{\rm min}$ range and the biggest change is seen near the local maximum of β^*, where β^* can improve from 4.5% to 5.9% when Δq increases from 0 to 0.35, at $q_{\rm min} \simeq 1.15$. The improvement in the ballooning β limit with Δq, is attributed to the increase of $\sqrt{\Psi_{\rm min}/\Psi_a}$, due to the prescibed current profile, which acts to broaden the second stable negative shear region and to increase the positive shear outside. However this effect is small because the main contribution is from an improved potential well in the low positive shear region which remains unchanged when Δq varies at a fixed $q_{\rm min}$.

The results for $q_a = 3.2$, when the total current is increased to $I_p/aB_0 \simeq 1.43$, are shown in Fig. 9. Here, $B_1 = B_7 = 0$, and $B_2 = -2B_4$ is used to change $q_{\rm min}$. It can be seen from Fig. 10 that Δq and $\sqrt{\Psi_{\rm min}/\Psi_a}$ (along the $r_{\rm wall} = 1.3$, $n = 1$ boundary of Fig. 9), is comparable to those in Fig. 3(a) of $q_a = 4.5$, where the amount of shear reversal is large. Qualitatively similar results to Figs. 2 and 5, are found in Fig. 9. The β^* limit reaches a maximum

of $\beta_t \simeq 3.6\%$, $\beta^* \simeq 5.6\%$ at $q_{\min} \simeq 1.34$, which is an increase of more than 30% from the low I_p/aB_0 case (Fig. 2), for the $n = 1$ mode without a wall. However, this increase is mainly due to the increased I_p/aB_0; i.e., β_N increases from 2.4 to 2.6. This differs from the broad pressure profile ($2.5 \leq P_f \leq 3$) results of Ref. [16], where β_N improves considerably when I_p/aB_0 is lowered. With a wall the maximum β is limited by the $n = 2$ mode to $\beta_t \simeq 4.7\%$, $\beta_N \simeq 3.2$ and $\beta^* \simeq 7.2\%$ at $q_{\min} \simeq 1.3$.

4 Conclusions

The ideal MHD β limits set by $n = 1$, 2, and ballooning modes have been investigated for a peaked pressure profile, of the type observed in JET reversed shear experiments [3, 7] with an internal transport barrier. This study is designed to improve physical insight into the stability of equilibria with reversed shear: a subject which has received considerable interest recently.

In summary, it has been found that when $q_{\min} \leq 1.25$ with $q_a = 4.5$, ballooning modes become unstable before $n = 1$, 2 modes, limiting further increase of the total pressure. The ballooning unstable region is located in low shear region just outside the $q_{\min}$ surface. The β limits due to $n = 1$, 2 modes reach local minima when the mode rational surface is just resonant (i.e., $q_{\min} \simeq m/n$), and reach local maxima in between. The effect of the wall on the stability of the $n = 1$ mode stability is more pronounced for higher $q_{\min}$, where the mode structure shows a greater contribution from large m components which have an external character. The conducting wall not only improves the β limit but also broadens the local maximum of β^*, thus reducing requirements for fine scale control of the current profile. The wall stabilisation is stronger for the $n = 1$ mode than the $n = 2$ mode, which is dominated by large internal $m = 2$, 3 components. When $q_{\min} \geq 1.25$,

the $n = 1$ mode is the most limiting unless a conducting wall is introduced to improve the $n = 1$ stability, or unless Δq becomes very small where the $n = 2$ mode becomes more unstable.

Increasing the amount of shear reversal is beneficial for all MHD modes considered and is more so for the $n = 2$ mode, though the effect saturates for $\Delta q \geq 0.5$. A tight fitting wall and large Δq has the combined effect on improving the β limit for the $n = 1$ mode for $q_{\min}$ away from integer values. For $I_p/aB_0 \simeq 1.1$, the highest $\beta_t \simeq 2.6\%$, $\beta_N \simeq 2.4$, and $\beta^* \simeq 4.2\%$ is acheived at $q_{\min} \simeq 1.3$ with $\Delta q \simeq 0.7$, which is stable for all MHD modes without the conducting wall. With $r_{\text{wall}} = 1.3$, it improves to $\beta_t \simeq 3.0\%$, $\beta_N \simeq 2.8$, and $\beta^* \simeq 5.0\%$. It is reported [13] that for a strongly shaped plasma, a moderately close wall greatly improves β_N for broad pressure profiles and more than cancels the possible reduction in fusion yield due to the broadness of the pressure.

Finally, at lower $q_a(= 3.2)$, the increase in the maximum β^* is mainly due to larger I_p/aB_0. The net improvement in normalised β^*, $\beta^*/(I_p/aB_0)$, is negligible and increases only with a close conducting wall.

The peaked pressure profile has relatively poor bootstrap current alignment, which is disadvantageous for steady-state operation of tokamak. It may become unstable to resistive interchange modes [18] in the reversed shear region, therefore limiting the pressure gradient in the core, although it is also necessary consider such modes in the long mean free path regime in large tokamaks [22]. This has not been considered in this work and further study is needed.

5 Acknowledgement

We would like to thank F. Söldner for useful comments and discussions. The UKAEA authors were jointly funded by UK Department of Trade and Industry and EURATOM. This research was supported in part by the Taegu University Research Grant 1998.

6 Figure Captions

Figure 1. Typical pressure and q profiles. Here, equilibria have $q_a = 4.5$, $q_{\min} = 1.34$ and are marginally stable to the $n = 1$ mode when $r_{\text{wall}} = 1.3$ with the parametrisation used in (a) Fig. 2, (b) Fig. 7 and (c) Fig. 8.

Figure 2. The limits of β^* due to the $n = 1$ mode as a function of $q_{\min}$. The effect of a conducting wall and experimental boundary shape (shown in inset), denoted by crosses, is also shown. Here, $q_a = 4.5$, and $B_1 = B_4 = B_6 = 0$ is used.

Figure 3. The amount and location of shear reversal ($\Delta q = q_0 - q_{\min}$ and $\sqrt{\Psi_{\min}/\Psi_a}$, where $\Psi_{\min}$ is the value of Ψ at the $q_{\min}$ surface) as a function of $q_{\min}$ along the $n = 1$ stability boundaries with $r_{\text{wall}} = 1.3$ in (a) Fig. 2, (b) Fig. 7, and (c) Fig. 8.

Figure 4. An eigenfunction plot of the perpendicular displacement for the $n = 1$ mode as a function of normalised minor radius, where the mode is marginally unstable without a conducting wall for (a) $q_{\min} \simeq 1.1$ and (b) $q_{\min} \simeq 1.4$.

Figure 5. The limits of β^* due to $n = 2$, and ballooning modes as a function of $q_{\min}$. Effect of conducting wall on $n = 2$ stability and the limit when 10% of surfaces are ballooning unstable are also shown.

Figure 6. An eigenfunction plot of the perpendicular displacement for the $n = 2$ mode as a function of normalised minor radius, where the mode is marginally unstable without a conducting wall for $q_{\min} \simeq 1.45$.

Figure 7. The limits of β^* due to $n = 1$, $n = 2$, and ballooning modes as a function of $q_{\min}$. The effect of a conducting wall on $n = 1$ stability is

also shown. Here, $q_a = 4.5$, and $B_1 = B_4 = B_7 = 0$ is used.

Figure 8. The limits of β^* due to $n = 1$, $n = 2$, and ballooning modes as a function of $q_{\min}$. The effect of a conducting wall on $n = 1$ stability is also shown. Here, $q_a = 4.5$, and $B_4 = B_7 = 0$, $B_2 = 4B_1$ is used.

Figure 9. The limits of β^* due to $n = 1$, $n = 2$, and ballooning modes as a function of $q_{\min}$. The effect of a conducting wall on $n = 1$ stability is also shown. Here, $q_a = 3.2$, and $B_1 = B_7 = 0$, $B_2 = -2B_4$ is used.

Figure 10. The amount and location of shear reversal as a function of $q_{\min}$ along the $n = 1$ stability boundary with $r_{\text{wall}} = 1.3$ in Fig. 9.

References

[1] Sykes, A. and Turner, M.F., in Contr. Fusion and Plasma Heating (Proc. 9th Eur. Conf. Oxford, 1979) European Physical Society, Geneva (1979) 161.

[2] Strait, E.J., et.al., Phys. Rev. Lett. **75** (1995) 4421.; Chu, M.S., et.al., Phys. Rev. Lett. **77** (1996) 2710.

[3] Sips, A.C.C., et.al., in Contr. Fusion and Plasma Physics (Proc. 24th Eur. Conf. Berchtesgaden, 1997), Vol. 21A, Part I, European Physical Society, Geneva (1997) 97.

[4] Levinton, F.M., et. al., Phys. Rev. Lett. **75** (1995) 4417.

[5] Koide, Y. and the JT-60 Team, Plasma Phys. **4** (1997) 1623.

[6] Huysmans, G.T.A., et.al., in Contr. Fusion and Plasma Physics (Proc. 24th Eur. Conf. Berchtesgaden, 1997), Vol. 21A, Part I, European Physical Society, Geneva (1997) 21.

[7] Luce, T.C., et.al., in Contr. Fusion and Plasma Physics (Proc. 24th Eur. Conf. Berchtesgaden, 1997), Vol. 21A, Part III, European Physical Society, Geneva (1997) 1105.

[8] Troyon, F., et.al., Plasma Phys. and Contr. Fusion **26** (1984) 209.

[9] Kotschenreuther, M., Bull. Am. Phys. Soc. **37** (1992) 1432.

[10] Kessel, C. et.al., Phys. Rev. Lett. **75** (1994) 1212.

[11] Phillips, M.W., et.al., Phys. Plasmas **3** (1996) 1673.

[12] Turnbull, A.D., et.al., in Fusion Energy (Proc. 16th Int. Conf. Montreal, 1996) Vol 2, IAEA, Vienna (1996) 509.

[13] Turnbull, A.D., et.al., submitted to Nucl. Fusion.

[14] Lee, B.J., et.al., Nucl. Fusion **37** (1997) 1271.

[15] Bonoli, P.T., et.al., Plasma Phys. Control. Fusion **39** (1997) 223.

[16] Bondeson, A., et.al., Nucl. Fusion **37** (1997) 1419

[17] Connor, J.W., Hastie, R.J., Taylor, J.B., Phys. Rev. Lett. **40** (1978) 396.

[18] Chu, M.S., et.al., Phys. Rev. Lett. **77** (1996) 2710.

[19] Huysmans, G.T.A., et.al., in Computational Physics (Proc.Conf. Amsterdam,1990), World Scientific Publishing, Singapore (1991) 371.

[20] Mikhailovskii, A.B., et.al., Plasma Phys. Rep. **23** (1997) 844.

[21] Turnbull, A.D., et.al., in Plasma Phys. and Contr. Nucl. Fusion Research (Proc. 15th Int. Conf. Seville, 1994) Vol 1, IAEA, Vienna (1995) 705.; Strait, E.J., et.al., Phys. Rev. Lett. **74** (1995) 2483.

[22] Connor, J.W. and Chen, L., Phys. Fluids **28** (1985) 2201.

Figure 1

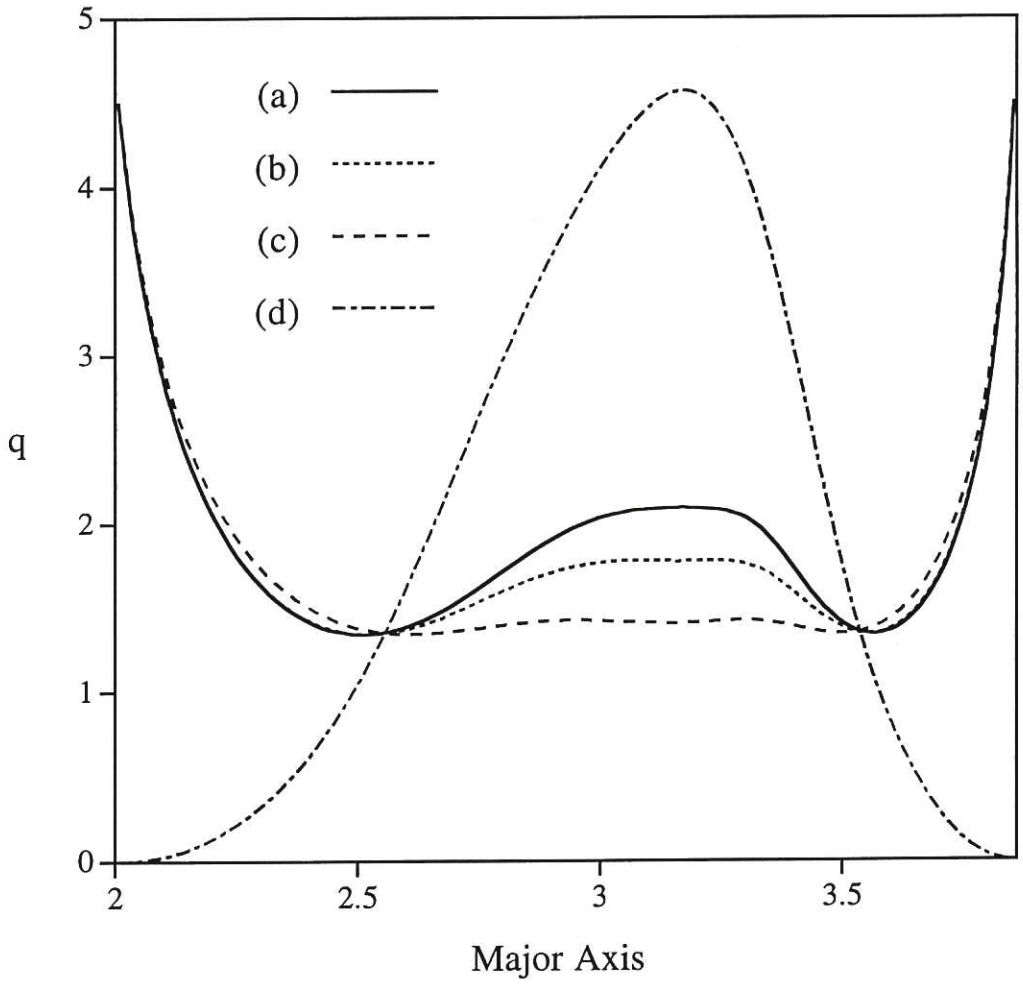

Figure 2

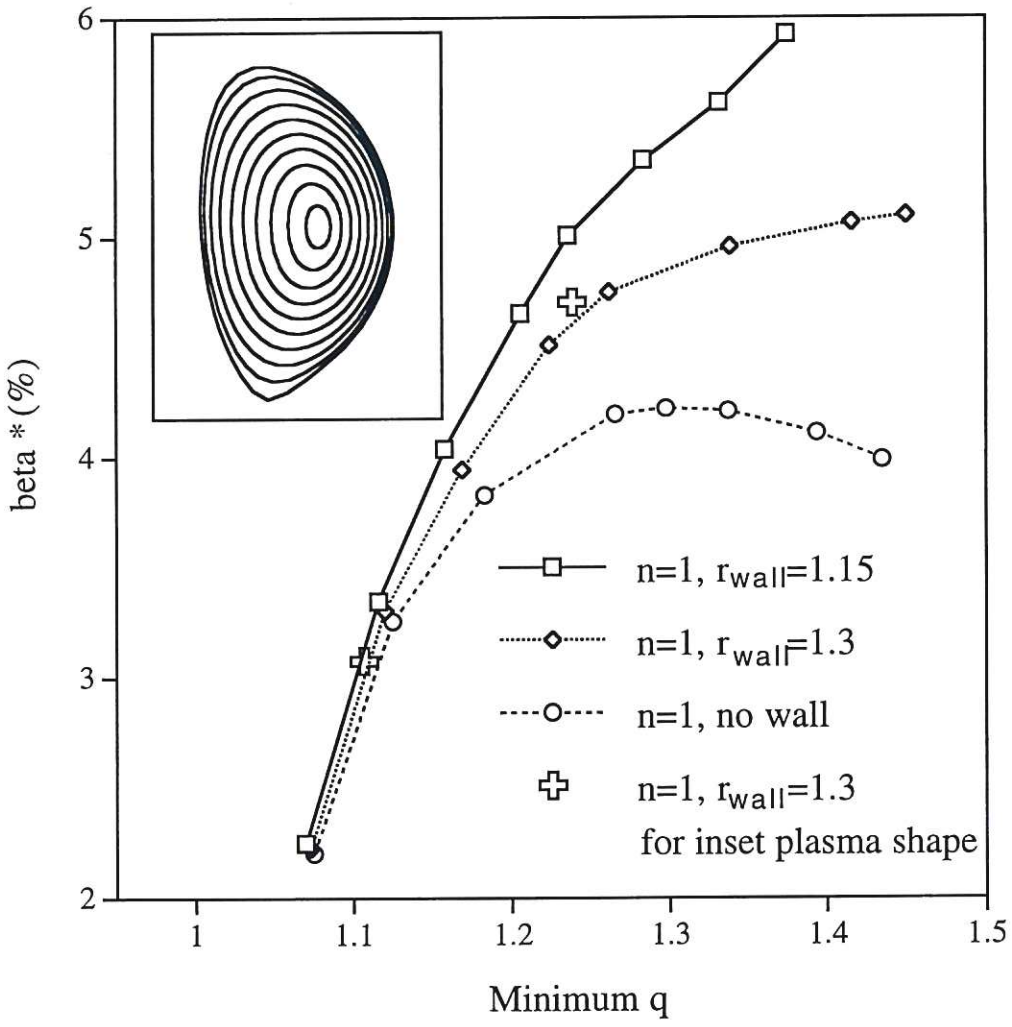
6
5
4
3
2
beta * (%)
1
1.1
1.2
1.3
1.4
1.5
Minimum q
n=1, r_wall=1.15
n=1, r_wall=1.3
n=1, no wall
n=1, r_wall=1.3
for inset plasma shape

Figure 3

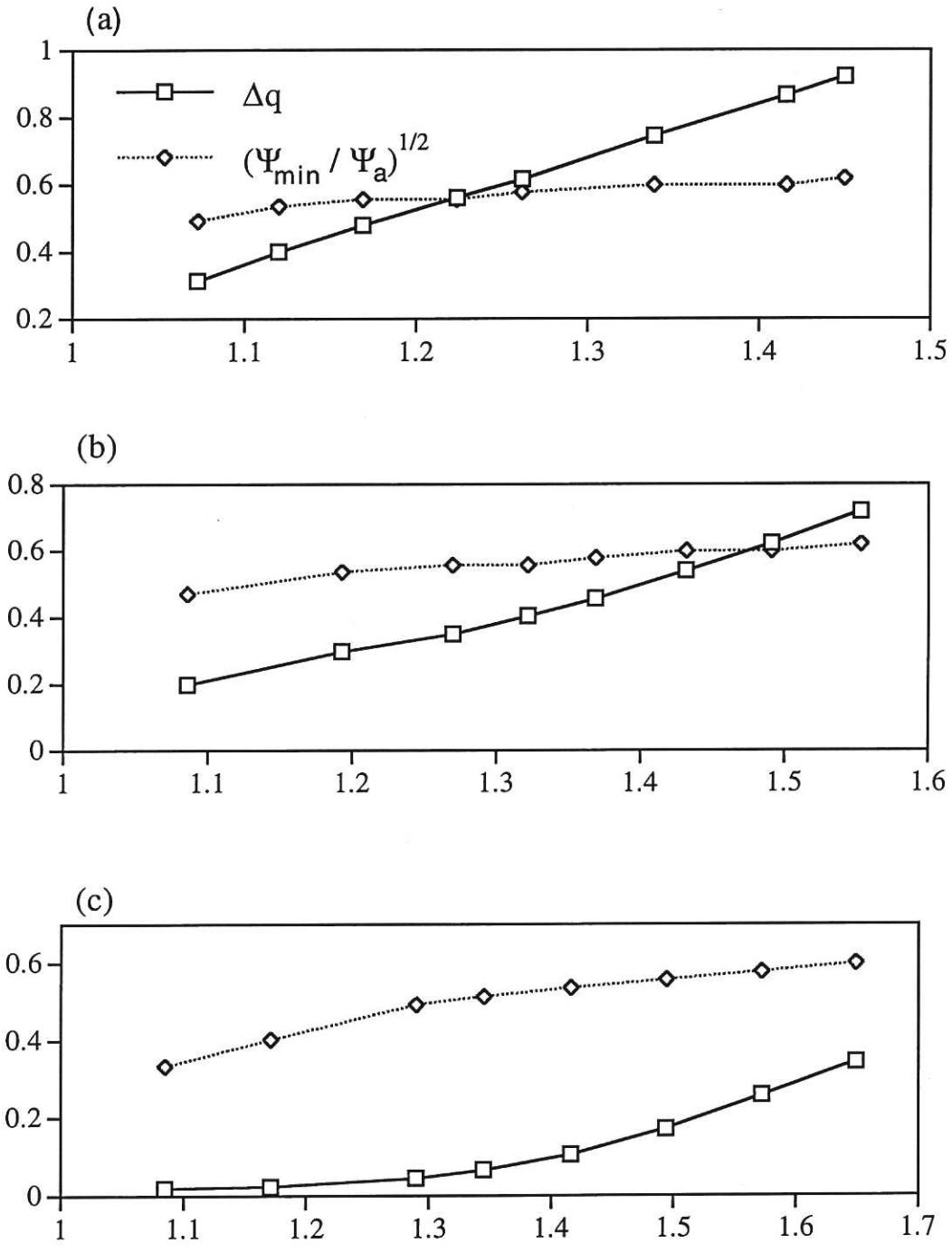

Figure 4(a)

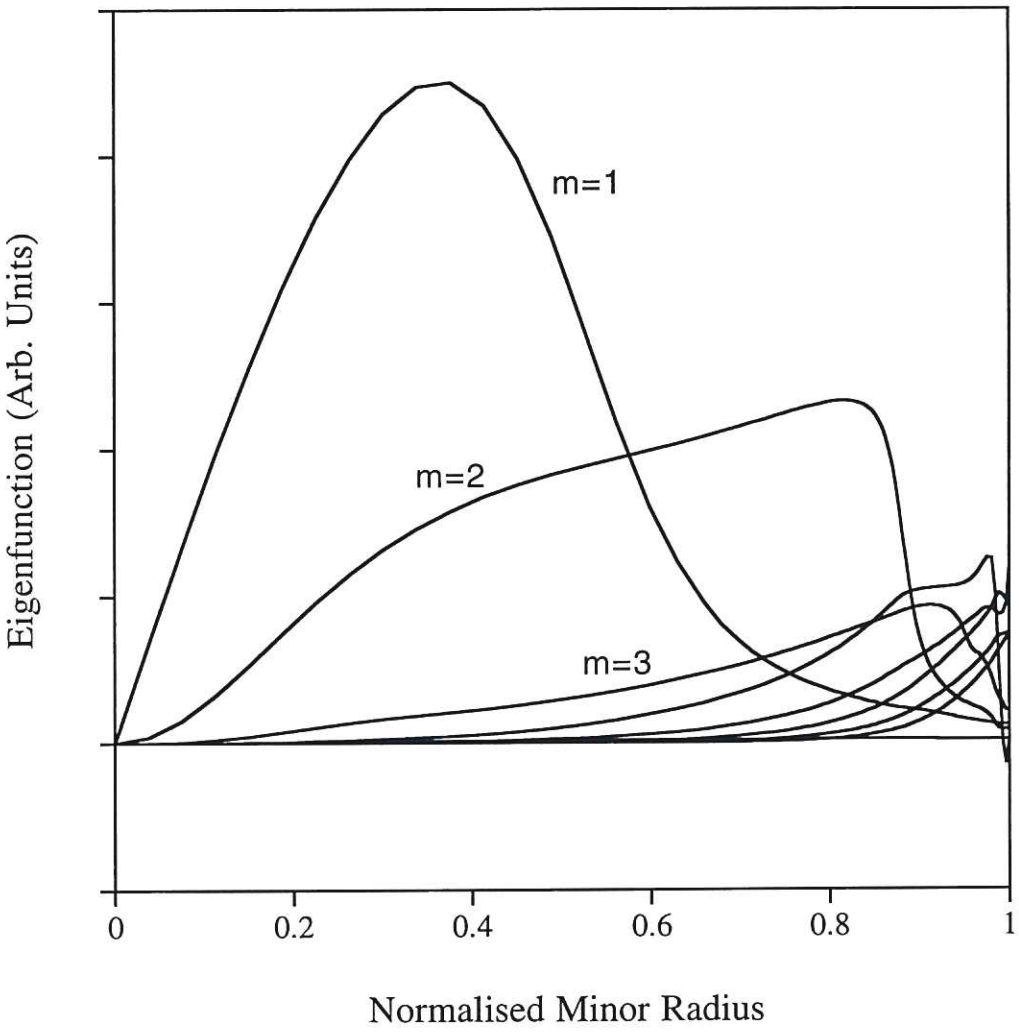
m=1
m=2
m=3
Eigenfunction (Arb. Units)
0
0.2
0.4
0.6
0.8
1
Normalised Minor Radius

Figure 4(b)

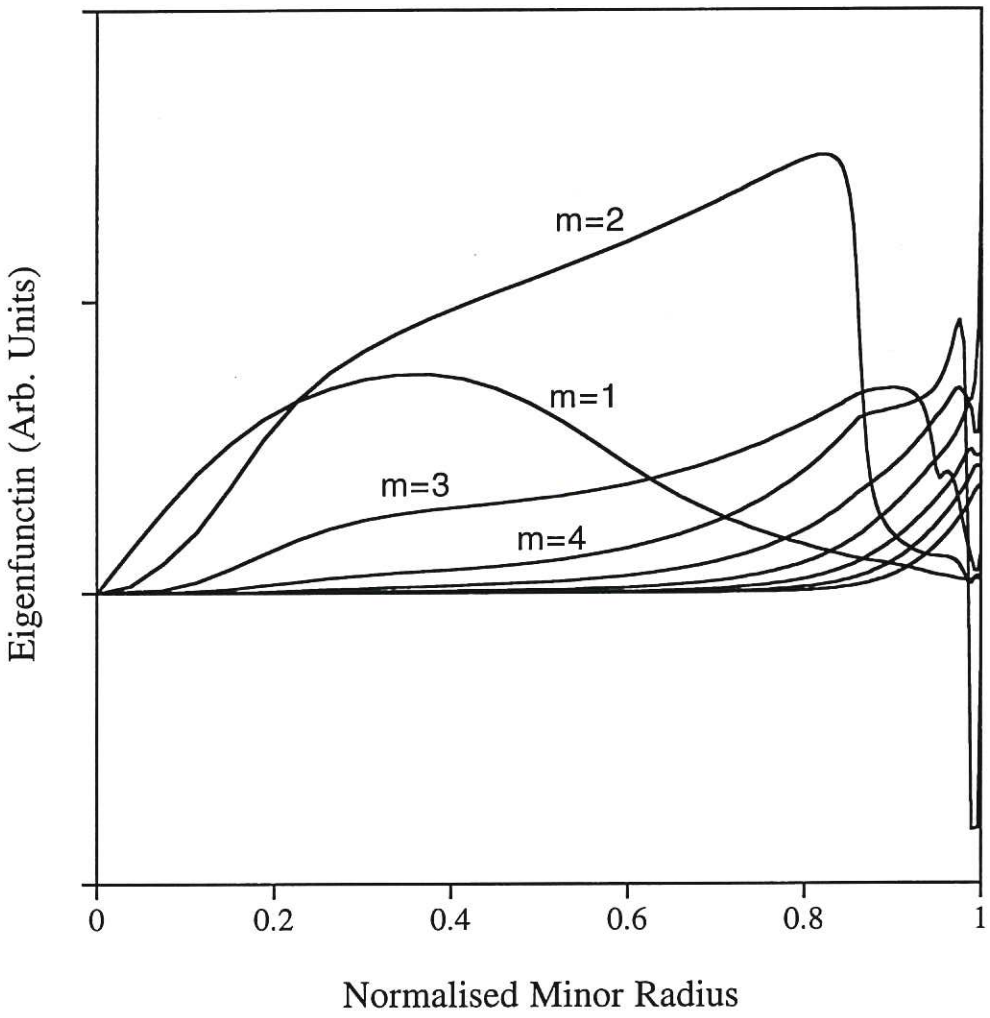
m=2
m=1
m=3
m=4
Eigenfunctin (Arb. Units)
0
0.2
0.4
0.6
0.8
1
Normalised Minor Radius

Figure 5

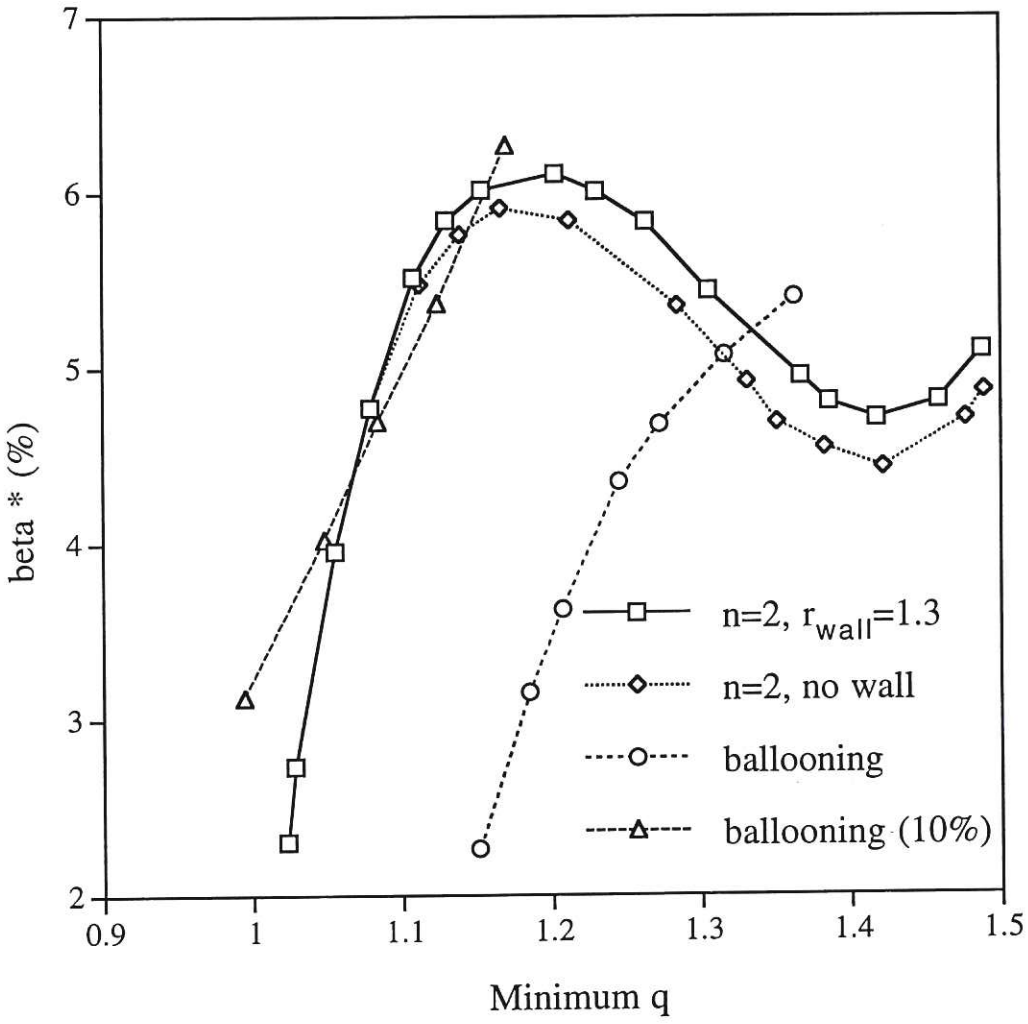
7
6
5
4
3
2
beta * (%)
0.9
1
1.1
1.2
1.3
1.4
1.5
Minimum q
n=2, r_wall=1.3
n=2, no wall
ballooning
ballooning (10%)

Figure 6

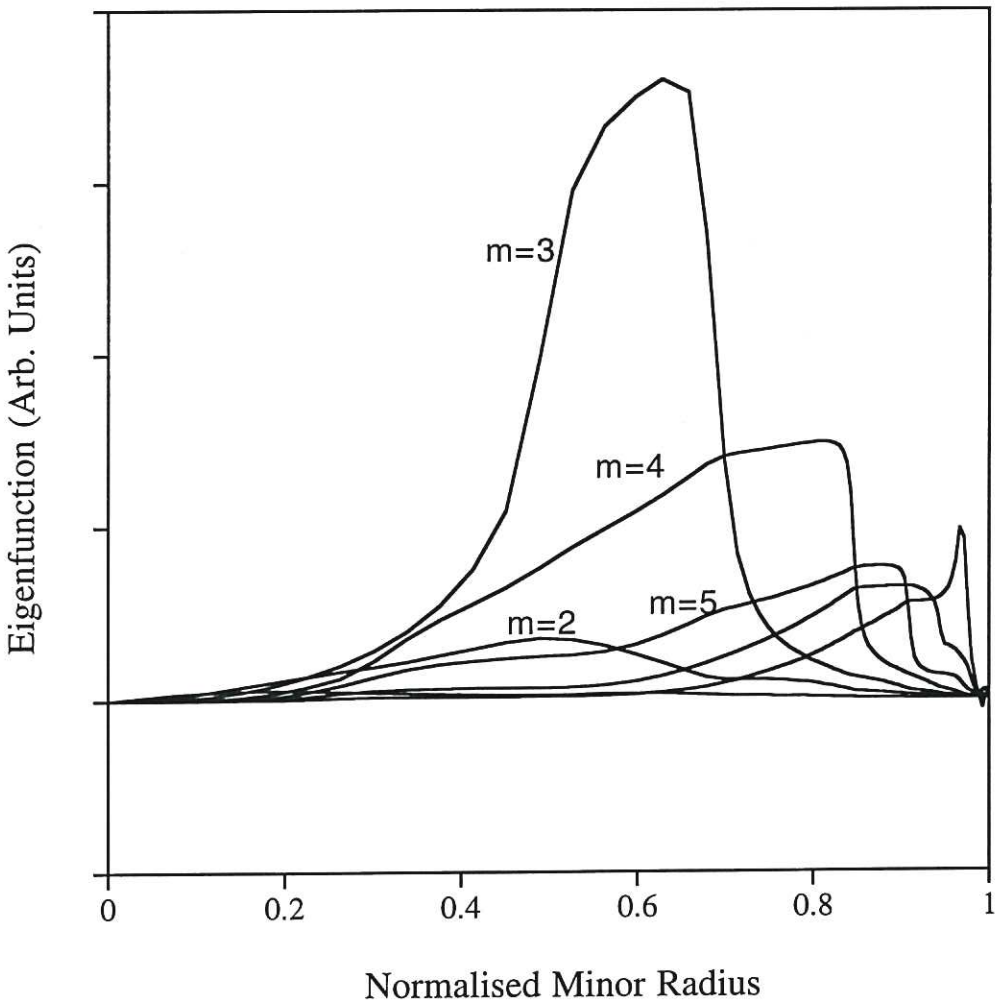
Eigenfunction (Arb. Units)
m=3
m=4
m=5
m=2
0
0.2
0.4
0.6
0.8
1
Normalised Minor Radius

Figure 7

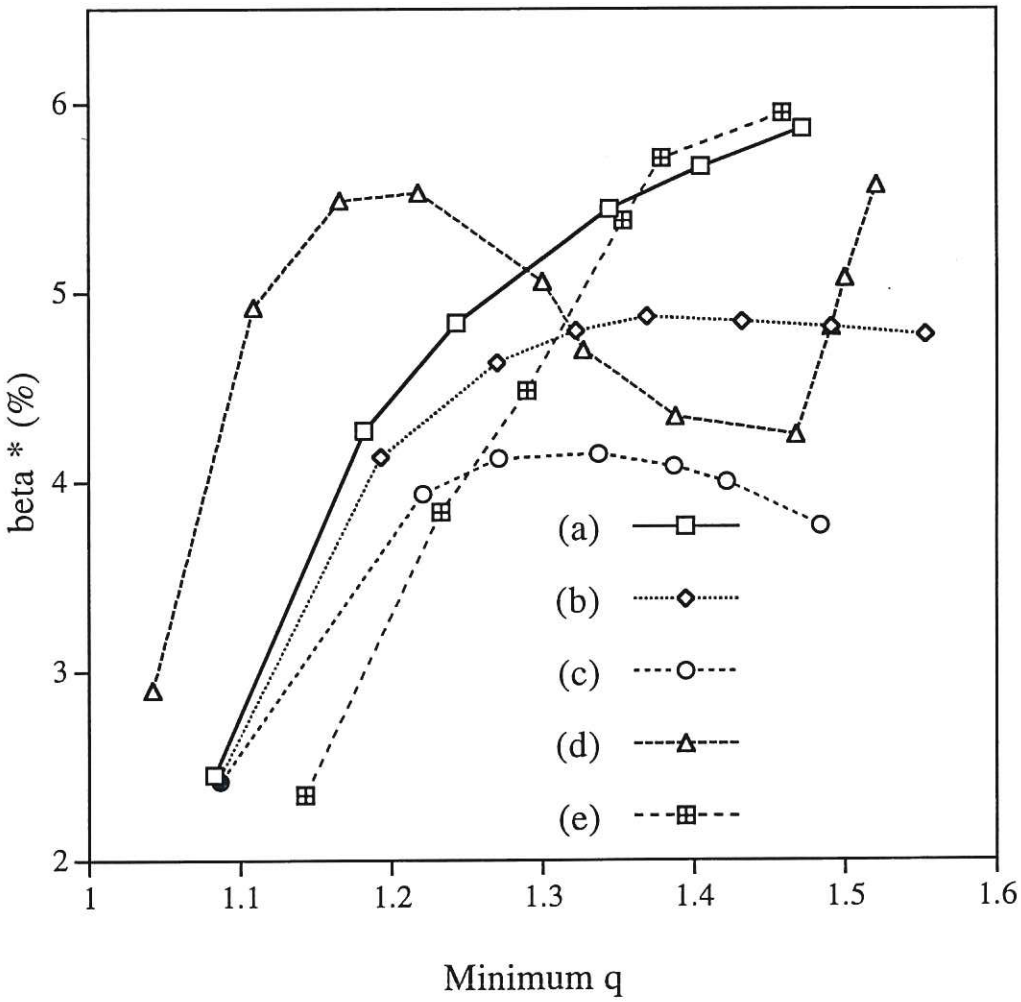

Figure 8

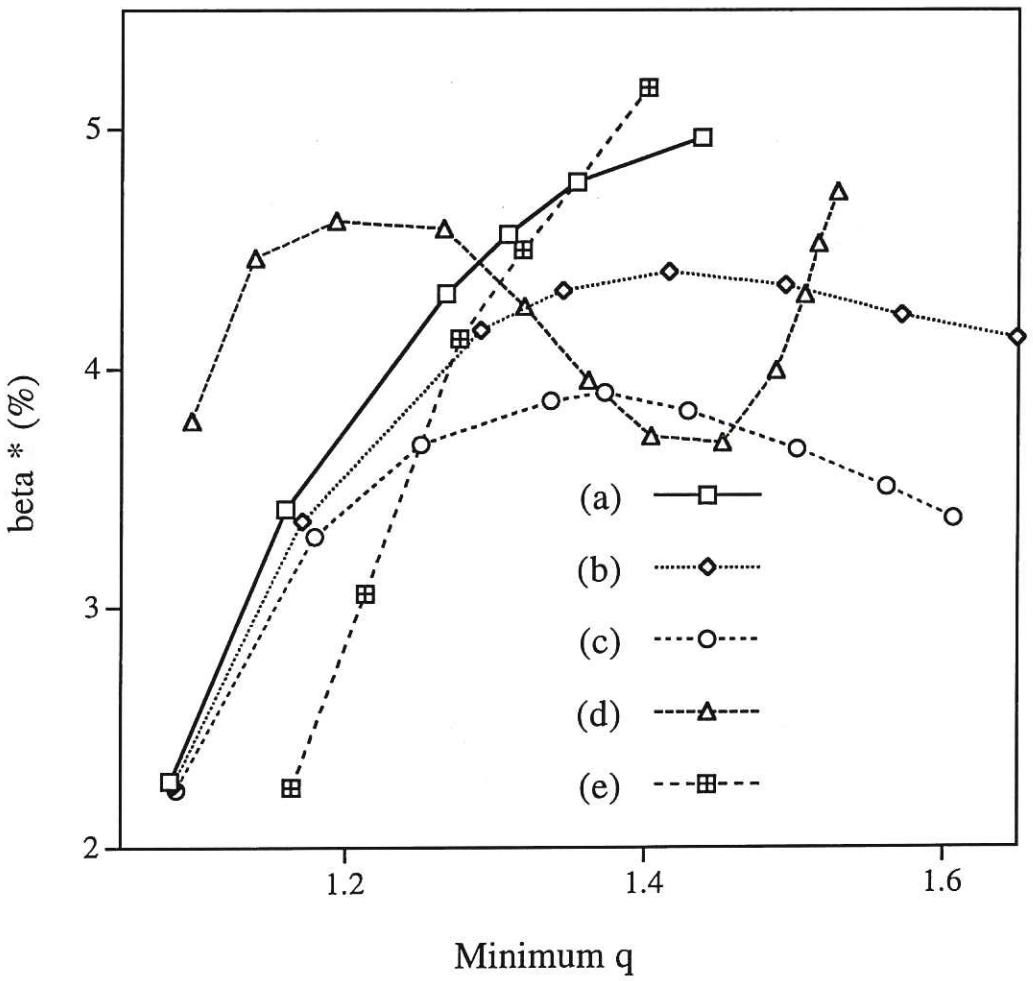

Figure 9

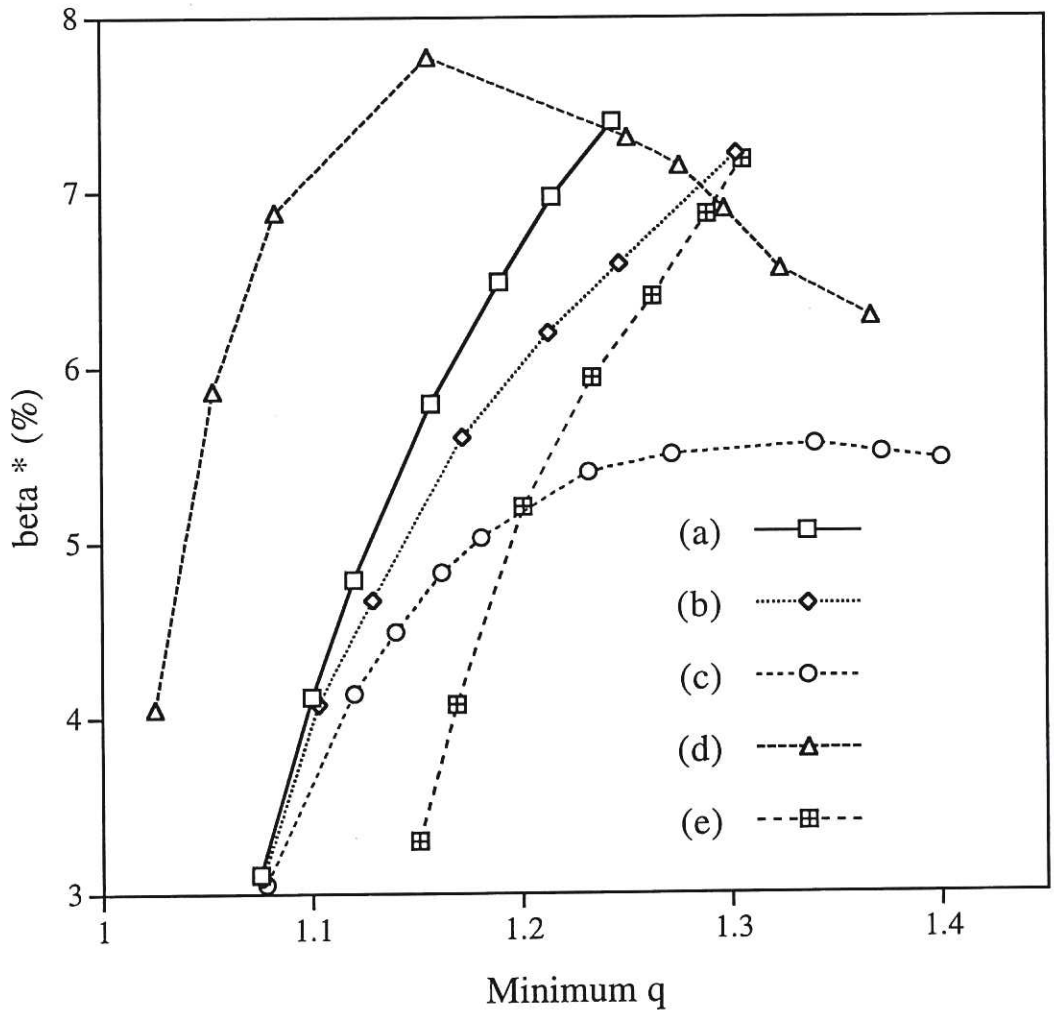

Figure 10